Author Manuscript

Author Manuscript

Author Manuscript

Author Manuscript

HHS Public Access

Author manuscript

*Nat Commun*. Author manuscript; available in PMC 2015 August 20.

Published in final edited form as:

*Nat Commun*. ; 6: 6200. doi:10.1038/ncomms7200.

# Protein kinase D1 drives pancreatic acinar cell reprogramming and progression to intraepithelial neoplasia

**Geou-Yarh Liou**[1], **Heike Döppler**[1], **Ursula B. Braun**[3], **Richard Panayiotou**[1], **Michele Scotti Buzhardt**[1], **Derek C. Radisky**[1], **Howard C. Crawford**[1], **Alan P. Fields**[1], **Nicole R. Murray**[1], **Q. Jane Wang**[2], **Michael Leitges**[3,4], and **Peter Storz**[1,4]

[1]Department of Cancer Biology, Mayo Clinic Comprehensive Cancer Center, Mayo Clinic, Jacksonville, FL 32224, USA

[2]Department of Pharmacology and Chemical Biology, University of Pittsburgh, Pittsburgh, PA 15260, USA

[3]The Biotechnology Centre of Oslo, University of Oslo, Oslo, Norway

## Abstract

The transdifferentiation of pancreatic acinar cells to a ductal phenotype (acinar-to-ductal metaplasia, ADM) occurs after injury or inflammation of the pancreas and is a reversible process. However, in the presence of activating Kras mutations or persistent epidermal growth factor receptor (EGF-R) signaling, cells that underwent ADM can progress to pancreatic intraepithelial lesions (PanINs) and eventually pancreatic cancer. In transgenic animal models, ADM and PanINs are initiated by high-affinity ligands for EGF-R or activating Kras mutations, but the underlying signaling mechanisms are not well understood. Here, using a conditional knockout approach, we show that Protein Kinase D1 (PKD1) is sufficient to drive the reprogramming process to a ductal phenotype and progression to PanINs. Moreover, using 3D explant culture of primary pancreatic acinar cells, we show that PKD1 acts downstream of TGFα and Kras to mediate formation of ductal structures through activation of the Notch pathway.

### Keywords

metaplasia; pancreas; acinar cells; Kras; Notch; dedifferentiation; PanIN

Users may view, print, copy, and download text and data-mine the content in such documents, for the purposes of academic research, subject always to the full Conditions of use:http://www.nature.com/authors/editorial_policies/license.html#terms

[4]Co-corresponding authors: Peter Storz, Mayo Clinic, Griffin Rm 306, 4500 San Pablo Road, Jacksonville, FL 32224, USA. Phone: 904 953-6909, storz.peter@mayo.edu. Michael Leitges, The Biotechnology Centre of Oslo, University of Oslo, Gaustadalleen 21, Oslo, N-0349, Norway. Phone: +47-22840572, michael.leitges@biotek.uio.no.

**Author contributions**

P.S. and G-Y.L. conceived and designed the experiments; G-Y.L., R.P. and H.D. performed the experiments; G-Y.L., H.D., R.P. M.L. and P.S. analyzed the data, M.L. and U.B. generated the PKD1$^{fl/fl}$ mice, G-Y.L., P.S., R.P., D.C.R., M.S.B., Q.J.W., N.R.M., A.P.F., H.C.C. contributed critical reagents, materials and analysis tools; and P.S. wrote the paper. All authors critically discussed the results, and reviewed and approved the manuscript before submission.

**Competing financial interests:**

The authors declare no competing financial interests.

Author Manuscript Author Manuscript Author Manuscript Author Manuscript

## INTRODUCTION

Approximately 95% of all pancreatic ductal adenocarcinoma (PDAC) express either somatic activating mutations of Kras [1] or show increased epidermal growth factor receptor (EGF-R) signaling [2, 3]. A pathological progression model for PDAC suggests that it originates from a duct-like progenitor cell type that gives rise to pancreatic intraepithelial neoplasia (PanIN) [4, 5, 6]. The use of genetic animal models provided evidence that most differentiated pancreatic epithelial cell types, including acinar cells, can transdifferentiate to the duct-like cell type that generates PanIN lesions [7, 8, 9]. Acinar-to-ductal metaplasia (ADM) is accompanied by altered gene expression including a decrease in acinar markers such as amylase or carboxypeptidase A or Mist-1 [10], and the acquisition of ductal markers such as cytokeratin-19 (CK-19) or mucin-1 [11]. However, cells that undergo ADM also show increased expression of Pdx1 (pancreatic and duodenal homeobox-1) [12], and the Notch targets Hes-1 (hairy and enhancer of split 1) and Hey-1 (hairy enhancer of split-related with YRPW motif protein-1) [13], indicating that this reprogramming process also leads to a less-differentiated, immature pancreatic cell type [5]. Mediators of ADM *in vivo* are activating mutations of Kras, inflammation and persistent activation of the EGF-R. For example, transgenic expression of the EGF-R ligand transforming growth factor α (TGFα) under the control of the elastase promoter can induce pancreatic metaplasia [14]. Moreover, in a transgenic animal model, in which an oncogenic mutant of Kras is expressed in acinar cells of the pancreas, ADM and progression to PanIN lesions are observed [7]. These events caused by mutated Kras are further potentiated and lead to pancreatic cancer, when additional pancreatic inflammation occurs [15, 16, 17, 18]. While such genetic animal models are ideal to provide insight into the contribution of molecules to organ pathology, such long-term studies make it difficult to investigate actual signaling mechanisms involved in the ADM process.

Signaling mechanisms that regulate the acinar-ductal transformation process can be studied in an *ex vivo* explant three dimensional (3D) cell culture model in which primary acinar cells are isolated from the pancreas and transdifferentiated in the presence of growth factors. For example, the epidermal growth factor receptor ligands TGFα and EGF can drive ADM *in vitro* [19, 20, 21, 22, 23]. Using a 3D explant model, and either PKD inhibitors or a PKD1 knockdown approach, we here provide evidence that the serine/threonine kinase Protein Kinase D1 (PKD1) is necessary for TGFα- and Kras-mediated formation of duct-like structures originating from acinar cells. Moreover, we show that active PKD1 is sufficient to drive this transdifferentiation process. We confirm the relevance of this signaling pathway *in vivo*, since the knockout of PKD1 in acinar cells of $p48^{cre}$;$Kras^{G12D}$ mice decreases the progression of ADM to PanIN lesions. Since acinar cell transformation and progression to PanIN lesions is one of the earliest known events contributing to the development of pancreatic cancer, our data suggest that pharmacologic inhibition of PKD may be an effective strategy to prevent early changes involved in development of pancreatic cancer.

## RESULTS

### PKD1 is upregulated in transforming acinar cells

Transformation of acinar cells to a duct-like phenotype and formation of PanINs can be observed *in vivo* in transgenic animals expressing TGFα or constitutively-active

Author Manuscript Author Manuscript Author Manuscript Author Manuscript

Kras [5, 14, 16, 24, 25]. Of the three PKD isoforms, PKD1, PKD2 and PKD3, acinar cells of normal pancreas only express PKD3 (Supplementary Fig. 1A and [26]). However, in transgenic mice that express TGFα in the pancreatic epithelium, in areas where acinar cells undergo ADM, the PKD expression pattern was altered (Fig. 1A). PKD1 showed increased expression in regions of ADM and PanIN lesions, but not in adjacent regions of "normal" acinar structures (Fig. 1A4). Of note, the cells forming these "normal" acinar structures also express the TGFα transgenic allele, but have not yet undergone transformation. The other two PKD isoforms, PKD2 and PKD3 were expressed in the more "normal" acinar structures of the TGFα transgenic mice, but in contrast to PKD1, their expression decreased in regions of ADM (Figs. 1A5 and 1A6). Upstream activating phosphorylations of PKD in regions of ADM was determined by IHC with a phosphospecific antibody that specifically recognizes PKD phosphorylated at the activation loop (labeled: anti-pS744/748-PKD). This antibody does not distinguish between PKD1, PKD2 and PKD3. However, staining with this antibody overlapped with PKD1 staining (Fig. 1A3), indicating that in ADM regions PKD1 is up-regulated and phosphorylated by its upstream kinases. At a later age these mice developed more significant areas of ADM and PanINs, which exhibited even more significant elevation in PKD1 expression (Fig. 1B).

To investigate a potential role for PKD isoforms in ADM, we next utilized an established explant model [22, 23], in which mouse primary pancreatic acinar cells are isolated and then reseeded *ex vivo* in 3D cell culture in Matrigel (extracellular matrix) to induce ADM. Duct-like structures formed after 5 days in culture showed expression of PKD1 as well as markers for both acinar cells (amylase) and ductal cells (CK-19), indicating their transdifferentiated or progenitor phenotype (Fig. 1C). PKD1 expression was observed only in freshly-developed ducts, but not in remaining acinar cells (Supplementary Fig. 1B top). Moreover, PKD was active in newly-formed ducts (Supplementary Fig. 1B, bottom). Thus, data obtained with this *ex vivo* model are in accordance with our *in vivo* data.

Next, we utilized a more defined explant model in which acinar cells are seeded in collagen I 3D culture and transdifferentiation is induced by TGFα [23, 27]. Primary acinar cells from mouse pancreas seeded in collagen undergo full ADM within approximately 5 days, when treated with TGFα (Fig. 1D). This was accompanied by increased PKD1 protein expression, while PKD2 and PKD3 were marginally or not expressed at days 3 and 5 (Fig. 1E). Increased expression of PKD1 correlated with a corresponding increase in PKD activity (Fig. 1E), as well as a decrease in acinar markers and an increase in ductal markers, such as amylase or CK-19, respectively (Supplementary Fig. 1C). Of note, short-term stimulation (up to 5 hours) of acinar cells with TGFα did not result in upregulation of PKD1 protein or activity (Supplementary Fig. 1D). Indeed, cells undergoing transdifferentiation to a duct-like phenotype showed up to 400-fold induction of PKD1 mRNA at days 3 and 5 (Fig. 1F), suggesting that upregulation of protein is regulated at the mRNA level.

## PKD is necessary for TGFα-mediated acinar cell metaplasia

To determine if upregulation of PKD1 expression and activity is simply correlative with ADM, or alternatively is causative for the process, we compared TGFα-induced ADM of mouse primary pancreatic acinar cells that were lentivirally-infected with control-shRNA or

Author Manuscript Author Manuscript Author Manuscript Author Manuscript

shRNA specifically-targeting PKD1. TGFα-induced formation of ductal structures was significantly-decreased to approximately 50% when PKD1 was knocked-down (Fig. 2A). This was observed with two different shRNA sequences for mouse PKD1 (mPKD1-shRNA#1 and mPKD1-shRNA#2). Moreover, TGFα-mediated effects on ADM were rescued by expression of exogenous human PKD1 that is not affected by the shRNA targeting mouse PKD1. Knockdown of PKD1 not only had effects on the numbers of ducts formed, but also affected their size. Depletion of PKD1 expression levels to approximately 50% (Supplementary Fig. 2A), not only led to a 50% reduction of TGFα-induced ADM events (Fig. 2B, left side), but, ducts formed were also smaller in size. For example, in the presence of PKD1-shRNA the average ductal area was 0.001 $mm^2$, whereas the average ductal diameter in the control counterparts was 0.0025 $mm^2$, as determined by analyzing 100 ducts of each condition for their ductal area (Fig. 2B, right side).

Since PKD1 protein is very stable and a full knockdown was not achieved, we additionally utilized the PKD-specific inhibitors kb-NB-142-70 and CRT0066101 to determine the role of PKD activity in formation of duct-like structures. Treatment of cells with either kb-NB-142-70 (Fig. 2C) or CRT0066101 (Supplementary Fig. 2C) completely blocked TGFα-mediated ADM in a dose-dependent manner without affecting cell viability (Supplementary Figs. 2B, 2C). Taken together, our results clearly indicate that PKD1 expression and activity are necessary for TGFα-mediated ADM, and contribute to duct formation and size.

In transgenic animal models, expression of active Kras in pancreatic cells can drive the formation of ADM and further progression to PanINs or cystic papillary lesions [7, 28, 29]. Therefore, we next tested if TGFα in our *ex vivo* explant model mediates its effects on ADM through active Ras proteins. Primary acinar cells treated with TGFα (short-term and long-term stimulation) showed an increase in active Ras as measured by pulldown assays using GST-Raf-RBD (Fig. 2D and Supplementary Fig. 2D). Such pulldown assays do not distinguish between the Ras isoforms that are activated by TGFα. However, specific knockdown of Kras in acinar cells using two different lentiviral shRNA constructs effectively-blocked TGFα-mediated duct formation (Fig. 2E). These data suggest that TGFα-induced ADM is mediated, in part, through activation of endogenous Kras.

## PKD is necessary for Kras-mediated acinar cell metaplasia

To further determine the role of PKD1 downstream of active Kras in the ADM process, we analyzed bi-transgenic $p48^{cre}$;$Kras^{G12D}$ mice that express mutant Kras in pancreatic epithelial cells for PKD1 expression. We found that expression of PKD1 is upregulated in regions of ADM and in PanINs (Fig. 3A). In order to recapitulate these results *in vitro*, we isolated acinar cells from LSL-$Kras^{G12D}$ mice and induced the expression of active Kras with an adenovirus harboring cre recombinase (Adeno-Cre), prior to 3D explant culture. Expression of active Kras in acinar cells led to a dramatic increase in ADM events (Fig. 3B), as well as upregulation of PKD1 expression and activity, similar to that previously observed in cells treated with TGFα (Fig. 3C).

As previously observed for TGFα, $Kras^{G12D}$-induced formation of ductal structures was significantly-decreased when PKD1 was knocked-down using two different shRNA sequences for mouse PKD1 (Fig. 3D). Effects on ADM were rescued by ectopic expression

Author Manuscript Author Manuscript Author Manuscript Author Manuscript

of human PKD1 that is not affected by the shRNA targeting mouse PKD1. Lentiviral expression of active TdTomato-tagged Kras ($Kras^{G12V}$) in normal acinar cells was also able to drive ADM, albeit less efficiently (we observed only a 2- to 3-fold increase in ADM events) (Fig. 3E, compare bars 1 and 4); and this was blocked by pharmacologic inhibition of PKD1 with Kb-NB-142-70 (Fig. 3E and Supplementary Fig. 3A). The difference in the extent of ADM events observed in cells from LSL-$Kras^{G12D}$ mice infected with Adeno-Cre virus as compared to cells from normal mice infected with lentivirus harboring a TdTomato-tagged $Kras^{G12V}$ may be due to the use of primary acinar cells from different pancreata in each experiment, indicating that the adenoviral system is more efficient in targeting acinar cells, or that the fluorescence-tag renders Kras less effective in mediating ADM. However, of importance, we show an increase in ADM events using two different approaches to increase expression of active Kras in pancreatic acinar cells. Taken together these data suggest that PKD1 acts downstream of active Kras in the ADM process.

To test if the signaling observed in 3D explant culture has relevance *in vivo*, we compared ADM and PanIN formation in $p48^{cre}$;$Kras^{G12D}$ mice to $p48^{cre}$;$Kras^{G12D}$; $PKD1^{-/-}$ mice, or respective controls. The knockout of PKD1 in pancreatic acinar cells significantly-decreased $Kras^{G12D}$-caused formation of PanIN lesions as judged by H&E staining, and IHC for claudin-18 (Fig. 3F, for additional controls see Supplementary Figs. 3D and 3F). While overall numbers of abnormal structures (ADM, PanINs all combined) were similar (Supplementary Fig. 3E), a more detailed analysis showed that the knockout of PKD1 delays the progression of ADM areas to PanINs (Fig. 3G).

## PKD1 drives formation of an immature ductal phenotype

Next we tested if PKD1 is sufficient to drive the formation of duct-like structures. For this purpose, we infected pancreatic primary acinar cells with a lentivirus expressing either wildtype PKD1, an active mutant (PKD1.CA, PKD1.S738E.S742E), or a kinase-dead version (PKD1.KD, PKD1.K612W). Introduction of wildtype PKD1 increased ADM events in 3D explant cell culture approximately 2-fold and constitutively-active PKD1 approximately 6-fold as compared to virus control or kinase dead PKD1 (Fig. 4A). However, ducts generated by active PKD1 were neither as large, nor as well developed as ducts obtained when metaplasia was induced with TGFα (Fig. 4B, compare to Fig. 2B). An average ductal area of 0.001 $mm^2$ was obtained after expression of active PKD1, which is approximately half the size of ducts obtained after TGFα treatment. This result indicates that although active PKD1 can drive the formation of ductal structures, additional TGFα-induced and probably PKD1-independent signaling is required for ducts to increase in size. There is also the possibility that the mutant does not fully reproduce the activity or localization of activated wildtype PKD1.

Cells isolated from explant culture showed an increase in ductal markers (CK-19 and mucin-1) and a decrease in the acinar marker amylase at the protein and mRNA levels, when PKD1.CA was expressed (Figs. 4C and 4D). We also analyzed samples for expression of Pdx1, an established marker for progenitor cells for endocrine and exocrine pancreatic cells. Pdx1 when expressed in the adult pancreas has been shown to drive de-differentiation of

Author Manuscript Author Manuscript Author Manuscript Author Manuscript

acinar cells to a more immature ductal cell type and to cause ADM [12, 13]. Expression of active PKD1 upregulated Pdx1 approximately 8-fold (Fig. 4D).

### The TGFα-Kras-PKD1 pathway acts through Notch

The Notch signaling pathway has been established as a driver of acinar cell reprogramming to a ductal phenotype [21, 27, 30]. Therefore, using a Notch Signaling PCR array we analyzed if expression of active PKD1 in acinar cells affects the expression of Notch target genes, or genes that regulate Notch (Fig. 5A). Genes downregulated in their expression more than 4-fold by active PKD1 included *Cbl* and *Sel1l*, both suppressors of Notch signaling. Genes upregulated more than 4-fold in their expression by active PKD1 encode Adam10, Adam17 and MMP7, all proteinases that have been shown previously to mediate Notch activation [21, 31]. Additionally, we found upregulation of mRNA for the indirect Notch targets PPARγ (*Pparg*) and NF-κB1 (*Nfkb1*) [32, 33]. In this assay active PKD1 also strongly upregulated mRNA expression of Hes-1, which is a direct target for Notch. Therefore, we next tested the involvement of the Notch pathway downstream of TGFα, Kras and PKD1. First, we tested if Notch acts downstream of PKD1. We found that formation of ductal structures induced by active PKD1 can be effectively-blocked, when Notch1 was knocked-down (Fig. 5B). This correlated with a decrease of expression of the Notch1 target Hes-1 (Supplementary Fig. 4A). Notch activity is regulated by cleavage at multiple levels [34]. Our data in Fig. 5A has shown that PKD1 upregulates proteinases that lead to S2 cleavage (Adam10, Adam17). In order to mediate Notch activity, this first cleavage is followed by a second cleavage mediated by the γ-secretase complex (S3 cleavage). S3 cleavage leads to generation of the NICD (Notch intracellular domain) fragment that translocates to the nucleus [34]. Expression of active PKD1 in pancreatic acinar cells undergoing transdifferentiation indeed led to generation of NICD (Fig. 5C). Inhibiting S3 cleavage using the γ-secretase inhibitors DAPT and R04929097 blocked PKD1-mediated formation of ductal structures further indicating that PKD1 acts through activation of Notch (Fig. 5D and Supplementary Fig. 4B). Moreover, expression of the Notch targets Hes-1 and Hey-1 was decreased to basal levels in presence of both γ-secretase inhibitors (Fig. 5E). Since Notch is not the only target for γ-secretase we also tested if a S3-cleaved Notch fragment can drive ADM. To test this we infected acinar cells with control virus or lentivirus harboring NICD. We found that NICD induced the formation of ductal structures approximately 2-fold (Fig. 5F), and this correlated with the upregulation of the ductal marker CK-19, the dedifferentiation marker Pdx1 and the Notch target Hes-1 (Supplementary Fig. 4C).

Next, we tested if inhibition of γ-secretase also blocks ADM induced by the upstream regulators of PKD1, mutant Kras and TGFα. Acinar cells from LSL-$Kras^{G12D}$ mice were infected with control virus or virus harboring cre recombinase to induce expression of $Kras^{G12D}$. Expression of $Kras^{G12D}$ induced the expression of Notch target genes Hes-1 and Hey-1 (Fig. 5G), indicating that NICD is formed. Therefore, we next tested if $Kras^{G12D}$-driven ADM is blocked by DAPT or R04929097. Both γ-secretase inhibitors decreased the formation of ductal-structures approximately 50% (Fig. 5H). Similar results were obtained when acinar cells were stimulated with TGFα. TGFα led to the upregulation of the Notch target genes Hes-1 and Hey-1 in a time dependent manner, indicating that Notch is activated

Author Manuscript Author Manuscript Author Manuscript Author Manuscript

by S3 cleavage (Fig. 5I). Consequently, blocking of S3 cleavage by γ-secretase inhibitors blocked TGFα-mediated formation of ductal structures in 3D explant culture (Fig. 5J).

In summary, our results show that PKD1 is necessary to mediate TGFα- and active Kras-induced reprogramming of pancreatic acinar cells to a duct-like phenotype that can give rise to PanIN lesions. Moreover, active PKD1, when expressed in acinar cells is sufficient to initiate and drive this process. As one of the mechanism that is used by TGFα-Kras-PKD1 to drive this we identify activation of the Notch signaling pathway (Fig. 5K).

## DISCUSSION

Increased TGFα and EGF signaling is frequently found in PDAC [2, 3]. Similarly, activating Kras mutations are present in over 95% of all PDACs, and at a smaller percentage in PanIN lesions at all stages [1]. Transgenic expression of TGFα or active Kras in mouse pancreas resulted in acinar-to-ductal metaplasia, convincingly demonstrating a role for these factors as inducers of the formation of duct-like cells and PanIN lesions *in vivo* [7, 17, 27]. Using an *ex vivo* explant 3D cell culture model in which primary pancreatic acinar cells are isolated and induced to undergo ADM and formation of ductal structures in presence of growth factors such as EGF or TGFα [19, 20, 21, 22, 23], we found that Kras is downstream of TGFα to drive ADM (Figs. 2D, 2E). This observation is important since activating Kras mutations have been described as inducers of ADM *in vivo* [7], but so far a role for active Kras in driving this process *ex vivo* was not well established. The fact that growth factors such as TGFα also utilize Kras to mediate ADM convincingly demonstrates that both pathways can converge at the level of Kras.

PKD1 previously was implicated in pancreatic cancer since it is overexpressed in patient samples [35], while in normal pancreas PKD1 is not expressed in the exocrine cells [26], but has a role in insulin secretion of islets [36]. In PDAC cell lines PKD1 contributes to cell proliferation and cell survival [35, 37, 38, 39, 40, 41, 42, 43]. Moreover, it was recently shown that inhibition of PKD decreases orthotopic growth of pancreatic tumor cell lines in mice [37]. We show here that PKD1 signaling can contribute to very early events that alter pancreas cellular plasticity. Our data suggest that elevated levels of active PKD1 in pancreatic acinar cells are sufficient to drive the formation of duct-like cells (Fig. 4). PKD1 is downstream of TGFα and active Kras to mediate formation of this cell type (Fig. 2A-C and Figs. 3D, 3E). Blockage of such signaling *in vivo* by knockout of PKD1 leads to decreased formation of PanIN lesions, which are based on this duct-like cell type (Figs. 3F, 3G). Since specific small molecule PKD inhibitors exist [37, 41, 44], PKD1 is a promising new target to prevent ADM and further progression to PanIN lesions. Previously it was shown that the transcription factor Prrx1b is induced during ADM to upregulate expression of Sox9 [45]. Sox9 in presence of oncogenic Kras functions as an accelerator of formation of premalignant lesions [46]. Moreover, Sox9-deficient acinar cells expressing $Kras^{G12D}$ can undergo persistent acinar-to-ductal metaplasia, but do not progress to PanINs [46]. Since knockout of PKD1 in acinar cells also allows $Kras^{G12D}$-mediated acinar cell metaplasia, but decreases further progression to PanIN lesions (Fig. 3G), a functional link between PKD1 and Sox9 may exist.

Author Manuscript Author Manuscript Author Manuscript Author Manuscript

Another possibility is a crosstalk of PKD1 signaling pathways with the phosphatidylinositol 3-kinase (PI3-K) pathway. For example, it was shown that the knockout of *Pten*, a negative regulator of PI3-K signaling, leads to expression of Pdx1 and the Notch target gene Hes-1 [47], both markers for an undifferentiated epithelial phenotype [9, 48]. Activation of PKD1 in pancreatic acinar cells also led to upregulation of Pdx1 and Hes-1. This suggested that PKD1 can promote dedifferentiation and reprogramming of pancreatic epithelial cells, which is believed to be one of the earliest events that can initiate pancreatic cancer. The Notch signaling pathway plays an important role during embryonic pancreas development, where it maintains an undifferentiated precursor cell type [48]. In the adult pancreas, the formation of duct-like cells induced by transgenic expression of TGFα is abolished when Notch activation is pharmacologically blocked [27]. Using explant cultures it was further shown that Notch signaling can induce ADM and results in the accumulation of undifferentiated precursor cells [7, 27].

Our results now suggest that PKD1 acts downstream of TGFα and Kras to regulate the formation of duct-like cells via the Notch pathway. Specifically, we find that active PKD1 induced the expression of Adam10, Adam17 and MMP-7, all metalloproteinases that activate Notch directly by S2 cleavage and were previously linked to PDAC. For example, increased Adam17 mRNA expression and proteolytic activity was detected in pancreatic cancer cell lines, patient samples for chronic pancreatitis, as well as tissues with PanIN3 lesions or PDAC [31, 49]. Similar was found for Adam10 in human tissue samples of chronic pancreatitis and PDAC [50]. Direct cleavage of Notch by MMP-7 leads to its activation and contributes to acinar-to-ductal transdifferentiation [21]. Our data further indicate that active PKD1 also leads to formation of an active cytoplasmic domain (NICD), a final activation step that is mediated through S3 cleavage by γ-secretases (Fig. 5C). Consequently, treatment with the γ-secretase inhibitors DAPT or R04929097, which block Notch S3 cleavage, led to a decrease of PKD1-, TGFα- and Kras-mediated expression of the Notch target genes Hes-1 and Hey-1, as well as decreased formation of ductal structures (Fig. 5D–J). Increased Hes-1 expression is a *bona fide* marker for development of pancreatic cancer, since it was found to be up-regulated in pre-neoplastic lesions and pancreatic cancers in humans and mice [2, 7].

In summary, understanding the signaling pathways that regulate the reprogramming of acinar cells to a duct-like cell type that can give rise to PanIN lesions is important for risk prognosis or early diagnosis of pancreatic cancer. Such knowledge also may be used for identifying targetable signaling molecules that allow prevention of progression, and even possibly phenotype reversion. Here we identify PKD1 as a key signaling protein downstream of EGF-R and Kras that drives the formation of such duct-like cells and is pharmacologically-targetable by novel small molecule PKD-specific inhibitors.

## METHODS

### Antibodies and Reagents

The anti-amylase and anti-β-actin antibodies were from Sigma-Aldrich (St Louis, MO), anti-cytokeratin-19 antibody from Leica Microsystems (Buffalo Grove, IL), anti-claudin-18 antibody from Invitrogen (Carlsbad, CA), anti-Ras antibody from Epitomics (Burlingame, CA), anti-GST and anti-GFP from Santa Cruz (Santa Cruz, CA), anti-activated Notch1

Author Manuscript Author Manuscript Author Manuscript Author Manuscript

antibody from Abcam (Cambridge, MA), anti-PKD1 from Antibodies-online Inc. (Atlanta, GA), anti-PKD2 from Acris Antibodies (San Diego, CA), anti-PKD3 antibody from Bethyl Laboratories (Montgometry, TX), and anti-pS744/748-PKD antibodies from Cell Signaling Technology (Danvers, MA) or Abcam. Recombinant human TGFα was purchased from Chemicon (Billerica, MA) and R&D Systems (Minneapolis, MN). Dexamethasone was from Sigma-Aldrich, soybean trypsin inhibitor and collagenase I from Affymetrix (Santa Clara, CA). Phenol red-free Matrigel and rat tail collagen I were from BD Biosciences (San Diego, CA). Hoechst 33342 was purchased from Invitrogen (Grand Island, NY). The PKD inhibitor CRT0066101 was from TOCRIS (Ellisville, MO) and kb-NB-142-70 was described previously [51]. The γ-secretase inhibitors DAPT and R04929097 were from Cellagen Technology (San Diego, CA).

## Viral Constructs

Adenovirus to express Cre recombinase (Adeno-Cre, Ad-CMV-Cre) was purchased from Vector Biolabs (Philadelphia, PA). A lentiviral construct (plasmid #17623, EF.hICN1.CMV.GFP) to express the intracellular domain of Notch (NICD) was from Addgene (Cambridge, MA). pLenti6.3/V5-GFP-PKD1, pLenti6.3/V5-GFP-PKD1.CA or pLenti6.3/V5-GFP-PKD1.KD were generated by amplifying previously-described human PKD1, PKD1.S738E.S742E or PKD1.K612W using the following primers: 5′-CTGGATCCATGAGCGCCCCTCCGGTC-3′ and 5′-CCGCTCGAGTTACTTGTACAGCTCGTC-3′. The amplicon was inserted into pLenti6.3/V5-TOPO vector (Invitrogen) via TOPO cloning. pLenti6.3/V5-Flag-TdTomato-Kras$^{G12V}$ was generated by amplifying a Flag-Kras$^{G12V}$ mutant using 5′-GCGGGATCCATGGACTATAAGGACGATGATGACAAAACTGAATATAAACTTGTGGTAGTT-3′ and 5′-GCGACTAGTCATAAATTACACACTTTGTCTTTGA-3′ as primers. The amplicon was inserted into pLenti6.3/V5-TOPO vector (Invitrogen) via TOPO cloning. TdTomato was amplified from pRSET-B-tdTomato (gift from R. Tsien, UCSD) using 5′-AAGGATCCGCAATGGTGAGCAAGGGC-3′ and 5′-TAGGATCCCTTGTACAGCTCGTC-3′ as primers and then inserted into pLenti6.3/V5-Flag-Kras$^{G12V}$ via BamHI restriction sites. The obtained plasmid was confirmed by PCR for the correct orientation of TdTomato. Lentiviral plasmids to knock down murine PKD1, Kras or Notch1 were purchased from Sigma-Aldrich. The hairpin sequences for mPKD1-shRNA#1 and mPKD1-shRNA#2 were CCGGGAGTGTTTGTTGTTATGGAAACTCGAGTTTCCATAACAACAAACACTCTTTTT and CCGGCCTTCAGCTTTAACTCCCGTTCTCGAGAACGGGAGTTAAAGCTGAAGGTTTTT, respectively. The hairpin sequences for murine Kras-shRNA were CCGGCAAGTAGTAATTGATGGAGAACTCGAGTTCTCCATCAATTACTACTTGTTTTTG (labeled as Kras-shRNA#1) and CCGGGTGTTGACGATGCCTTCTATACTCGAGTATAGAAGGCATCGTCAACACTTTTTG (labeled as Kras-shRNA#2). The hairpin sequences for murine Notch1-shRNA were 5′-CCGGGCCAGGTTATGAAGGTGTATACTCGAGTATACACCTTCATAACCTGGCTTTTT-3′ (labeled as mNotch1-shRNA#1) and 5′-

Author Manuscript Author Manuscript Author Manuscript Author Manuscript

CCGGGCAGATGATCTTCCCGTACTACTCGAGTAGTACGGGAAGATCATCTGCTT TTT-3′ (labeled as mNotch-shRNA#2).

## Genetic Animal Models

MT-TGFα mice in a C57Bl/6 background were kept on 10 mM $ZnSO_4$ in the drinking water to induce the TGFα transgene. LSL-$Kras^{G12D}$ mice (obtained from the NCI Mouse Repository; MMHCC) were crossed with $p48^{cre}$ mice (a gift from Dr. Pinku Mukherjee, University of North Carolina) to generate bi-transgenic $p48^{cre}$;LSL-$Kras^{G12D}$ mice. A detailed scheme of the strategy to generate mice with an acinar cell-specific knockout of PKD1 as well as a representative genotyping and analysis are shown in Supplementary Figs. 3B, 3C and 3F. The PKD1 targeted allele (PKD1 gene locus upon homologous recombination of the targeting vector) was crossed into a mouse line ubiquitously expressing Flip to obtain the mouse line with PKD1 floxed allele. PKD1 floxed mice were crossed with $p48^{cre}$ mice to obtain mice with acinar cell specific knockout of PKD1 ($p48^{cre}$;$PKD1^{-/-}$ mice). Then, LSL-$Kras^{G12D}$ mice were crossed with $PKD1^{fl/fl}$ mice to generate LSL-$Kras^{G12D}$;$PKD1^{fl/fl}$ mice. Eventually, $p48^{cre}$;$PKD1^{-/-}$ mice were crossed with LSL-$Kras^{G12D}$;$PKD1^{fl/fl}$ mice to obtain $p48^{cre}$;$Kras^{G12D}$;$PKD1^{-/-}$ mice. All animal experiments performed were in compliance with ethical regulations and were approved by the Mayo Clinic Institutional Animal Care and Use Committee (IACUC).

## Isolation of Primary Pancreatic Acinar Cells and 3D Culture

The procedure to isolate primary pancreatic acinar cells was described in detail previously [18]. In brief, the pancreas was removed, washed twice with ice-cold HBSS media, minced into 1 – 5 mm pieces and digested with collagenase I (37 °C, shaker). Collagen digestion was stopped by adding an equal volume of ice-cold HBSS media containing 5% FBS. The digested pancreatic pieces were washed twice with HBSS media containing 5% FBS and then pipetted through 500 μm and then 105 μm meshes. The supernatant of the cell suspension containing acinar cells was dropwise added to 20 ml HBSS containing 30% FBS. Acinar cells were then pelleted (1000 rpm, 2 min, at 4 °C) and re-suspended in 10 ml Waymouth complete media (1% FBS, 0.1 mg $ml^{-1}$ trypsin inhibitor, 1 μg $ml^{-1}$ dexamethasone).

For the 3D explant culture [21, 22, 23], cell culture plates were coated with collagen I in Waymouth media w/o supplements. Isolated primary pancreatic acinar cells were added as a mixture with collagen I/Waymouth media on the top of this layer. Further, Waymouth complete media was added on top of the cell/gel mixture, replaced the following day and then every other day. When growth factors or inhibitors were added, the compound of interest was added to both, the cell/gel mixture and the media on top. To express proteins using adeno- or lentivirus, acinar cells were infected with virus of interest and incubated for 3 – 5 hours before embedding in the collagen/waymouth media mixture. At day 5 – 7 (dependent on time course of duct formation) numbers of ducts were counted under a microscope and photos were taken to document structures. The area of ducts was measured using Image J software and StatsDirect (StatsDirect Ltd; http://www.statsdirect.com) to obtain a distribution curve.

Author Manuscript Author Manuscript Author Manuscript Author Manuscript

### Determination of Cell Viability

Cellular viability was assessed using Hoechst 33342 without fixation step (staining of cells that are alive). Therefore, the media on top of the 3D culture were removed, the mixture of cell/collagen was rinsed twice with PBS and incubated with Hoechst 33342 (2.5 μg $ml^{-1}$ in PBS) at 37 °C for 30 min. After 3 washes in PBS, Hoechst 33342-stained cells were visualized using a DAPI filter with an Olympus IX71 fluorescent microscope, 10x magnification and DP70 digital camera.

### Measurement of Ras Activity

Ras activity was assessed using Raf-1-RBD pull-down assays. In brief, freshly isolated acinar cells were treated with 100 ng $ml^{-1}$ TGFα for indicated times. Cells were lysed with Buffer A (50 mM Tris/HCl pH 7.4, 1% TritonX-100, 150 mM NaCl, 5 mM EDTA) plus protease inhibitor cocktail (PIC, Sigma-Aldrich). Clarified cellular lysates were incubated with 20 μg GST-Raf-1-RBD (aa1-149) for 90 min at 4 °C followed by 3 washes with Buffer A. Samples were run on SDS-PAGE, transferred to nitrocellulose and analyzed for Ras (anti-Ras antibody). Input was controlled by staining with α-GST antibodies (GST-Raf-1-RBD input) or by staining of lysates for total Kras or β-actin.

### Immunohistochemistry

Slides were de-paraffinized (1 hr, 60° C), de-waxed in xylene (5 times, 4 min) and gradually re-hydrated with ethanol (100%, 95%, 75%, each 2 times, 3 min). Re-hydrated samples were rinsed in water and subjected to antigen retrieval in 10 mM sodium citrate buffer pH 6.0 (DAKO, Carpinteria, CA). Slides were treated with 3% $H_2O_2$ (5 min) to reduce endogenous peroxidase activity, washed with PBS containing 0.5% Tween 20, and blocked with protein block serum free solution (DAKO) for 5 min at RT. Samples were stained with H&E, alcian blue, anti-claudin-18 antibody (1:1000), anti-PKD1 antibody (1:100), anti-PKD2 antibody (1:200), anti-PKD3 antibody (1:200), or anti-pS744/748-PKD antibody (Abcam) at a dilution of 1:50 in Antibody Diluent Background Reducing Solution (DAKO) and visualized using the Envision Plus Dual Labeled Polymer Kit (DAKO) according to the manufacturer's instructions. Images were captured using the ScanScope XT scanner and ImageScope software (Aperio, Vista, CA).

### Immunostaining and Confocal Microscope Imaging

Freshly-isolated acinar cells were plated in phenol red-free Matrigel on top of a pre-coated chamber glass slide. Phenol red-free Waymouth complete media was added to the top of the polymerized Matrigel/acinar cell mixture. After duct formation cells were fixed with 4% formaldehyde in PBS for 20 min at RT, permeabilized with 0.5% TritonX-100 in PBS for 30 min at RT, washed 3 times with PBS and blocked with 10% goat serum in PBS cells for 1 hour at RT. Samples were incubated with primary antibodies (anti-PKD1 at 1:500; anti-CK-19 at 1:200; anti-amylase at 1:300) at 4 °C for overnight. Samples were washed 3 times with PBS containing 0.2% TritonX-100. Secondary antibodies (Alexa Fluor 546 goat-anti-rabbit from Invitrogen at 1:500) were added for 1 hour at RT. Samples were washed with PBS for 3 times. Images were captured using a LSM 510META confocal laser scanning microscope (Zeiss) with a 20x objective lens.

Author Manuscript Author Manuscript Author Manuscript Author Manuscript

### RNA Isolation and Quantitative Real-time PCR

Cells were harvested from explant 3D collagen culture by digestion in a 1 mg $ml^{-1}$ collagenase solution at 37 °C for 30 min on a shaker. Cells were washed once with HBSS and twice with PBS and total RNA isolation was performed using the miRCURY™ RNA isolation kit (Exiqon, Woburn, MA), and the TURBO DNA-free kit (Ambion, Austin, TX) to eliminate residual genomic DNA. mRNA of interest was assessed using a 2-step quantitative reverse transcriptase-mediated real-time PCR (qPCR) method. Equal amount of total RNA was converted to cDNA by the high capacity cDNA reverse transcriptase kit (Applied Biosystems, Bedford, MA). Quantitative PCR was performed in a 7900HT Fast real time thermocycler (Applied Biosystems) using the TaqMan Universal PCR master mix (Applied Biosystems) with probe/primer sets and the following thermocycler program: 95 °C for 20 sec; 40 cycles of 95 °C for 1 sec and 60 °C for 20 sec. All probe/primer sets were purchased from Applied Biosystems (PKD1: Mm00435790_m1; Pdx1: Mm00435565_m1; CK-19: Mm00492980_m1; mucin-1: Mm00449604_m1; Mist-1: Mm00627532_s1; Hes-1: Mm01342805_m1; Hey-1: Mm00468865_m1; GAPDH: Mm99999915_g1; 18S rRNA: Hs99999901_s1). The amplification data were collected by a Prism 7900 sequence detector and analyzed with Sequence Detection System software (Applied Biosystems). Data were normalized to murine GAPDH or 18s RNA, and mRNA abundance was calculated using the $\Delta\Delta C_T$ method. Quantitative real-time PCR with the mouse Notch Signaling Targets PCR Array from SA Biosciences (Frederick, MD) was carried out according to the manufacturer's instructions and data were analyzed with the web-based $RT^2$ Profiler PCR Array software (SA Biosciences).

### Cellular Extracts and Immunoblotting

Cells were harvested from explant 3D collagen culture by digestion in a 1 mg $ml^{-1}$ collagenase solution at 37 °C for 30 min on a shaker. Cells were washed once with HBSS, twice with PBS and lysed in Buffer A (50 mM Tris/HCl pH 7.4, 1% TritonX-100, 150 mM NaCl, 5 mM EDTA) supplemented with Protease Inhibitor Cocktail (Sigma). Lysates were incubated on ice for 30 min, centrifuged (13,000 rpm, 15 min, 4 °C), and supernatants were subjected to SDS-PAGE. Gels were either stained by silver gel staining (Pierce silver stain kit, Thermo Scientific), or resolved proteins were transferred to nitrocellulose membranes. Membranes were blocked with 5% BSA in TBST (50 mM Tris/HCl, pH 7.4, 150 mM NaCl, 0.1% Tween 20) and incubated with primary antibodies of interest in 5% BSA in TBST over night at 4 °C and then with horseradish peroxidase-conjugated secondary antibodies for 1 hour at RT. Samples were visualized with ECL and X-ray film (Supplementary Fig. 5).

### Statistical Analysis

Data are presented as mean ± standard deviation (s. d.). P values were acquired with the student's *t*-test using Graph Pad software, and $p < 0.05$ is considered statistically significant.

## Supplementary Material

Refer to Web version on PubMed Central for supplementary material.

Author Manuscript Author Manuscript Author Manuscript Author Manuscript

## Acknowledgments

We thank our colleagues in the Storz laboratory for helpful discussions. We also thank Brandy H. Edenfield (Cancer Biology Histology Facility) for IHC. This work was supported by grants from the AACR (08-20-25-STOR), the NIH (CA135102, GM86435, CA140182) and a Pilot Project from the Mayo Clinic SPORE for Pancreatic Cancer (P50CA102701) – all to PS, a grant from the Norwegian Research Council (grant: 197261) to ML, as well as CA122086 (DCR), CA142580 (QJW), CA136754 (HCC), CA140290 (NRM), CA081436 (APF). The content is solely the responsibility of the authors and does not necessarily represent the official views of the National Cancer Institute or the National Institutes of Health. The funders had no role in study design, data collection and analysis, decision to publish, or preparation of the manuscript. We thank the Pancreatic Cancer Action Network (PanCAN) and the Boshell Foundation for their support.

## References

1. Bardeesy N, DePinho RA. Pancreatic cancer biology and genetics. Nat Rev Cancer. 2002; 2:897–909. [PubMed: 12459728]
2. Hruban RH, Wilentz RE, Goggins M, Offerhaus GJ, Yeo CJ, Kern SE. Pathology of incipient pancreatic cancer. Ann Oncol. 1999; 10 (Suppl 4):9–11. [PubMed: 10436775]
3. Korc M. Role of growth factors in pancreatic cancer. Surg Oncol Clin N Am. 1998; 7:25–41. [PubMed: 9443985]
4. Hruban RH, et al. Pancreatic intraepithelial neoplasia: a new nomenclature and classification system for pancreatic duct lesions. Am J Surg Pathol. 2001; 25:579–586. [PubMed: 11342768]
5. Morris, JPt; Wang, SC.; Hebrok, M. KRAS, Hedgehog, Wnt and the twisted developmental biology of pancreatic ductal adenocarcinoma. Nat Rev Cancer. 2010; 10:683–695. [PubMed: 20814421]
6. Murtaugh LC, Leach SD. A case of mistaken identity? Nonductal origins of pancreatic “ductal” cancers. Cancer Cell. 2007; 11:211–213. [PubMed: 17349578]
7. Hingorani SR, et al. Preinvasive and invasive ductal pancreatic cancer and its early detection in the mouse. Cancer Cell. 2003; 4:437–450. [PubMed: 14706336]
8. Morris, JPt; Cano, DA.; Sekine, S.; Wang, SC.; Hebrok, M. Beta-catenin blocks Kras-dependent reprogramming of acini into pancreatic cancer precursor lesions in mice. J Clin Invest. 2010; 120:508–520. [PubMed: 20071774]
9. Carriere C, Seeley ES, Goetze T, Longnecker DS, Korc M. The Nestin progenitor lineage is the compartment of origin for pancreatic intraepithelial neoplasia. Proc Natl Acad Sci U S A. 2007; 104:4437–4442. [PubMed: 17360542]
10. Pin CL, Rukstalis JM, Johnson C, Konieczny SF. The bHLH transcription factor Mist1 is required to maintain exocrine pancreas cell organization and acinar cell identity. J Cell Biol. 2001; 155:519–530. [PubMed: 11696558]
11. Strobel O, et al. In vivo lineage tracing defines the role of acinar-to-ductal transdifferentiation in inflammatory ductal metaplasia. Gastroenterology. 2007; 133:1999–2009. [PubMed: 18054571]
12. Song SY, et al. Expansion of Pdx1-expressing pancreatic epithelium and islet neogenesis in transgenic mice overexpressing transforming growth factor alpha. Gastroenterology. 1999; 117:1416–1426. [PubMed: 10579983]
13. Miyatsuka T, et al. Persistent expression of PDX-1 in the pancreas causes acinar-to-ductal metaplasia through Stat3 activation. Genes Dev. 2006; 20:1435–1440. [PubMed: 16751181]
14. Sandgren EP, Luetteke NC, Palmiter RD, Brinster RL, Lee DC. Overexpression of TGF alpha in transgenic mice: induction of epithelial hyperplasia, pancreatic metaplasia, and carcinoma of the breast. Cell. 1990; 61:1121–1135. [PubMed: 1693546]
15. Logsdon CD, Ji B. Ras activity in acinar cells links chronic pancreatitis and pancreatic cancer. Clin Gastroenterol Hepatol. 2009; 7:S40–43. [PubMed: 19896097]
16. Guerra C, et al. Pancreatitis-induced inflammation contributes to pancreatic cancer by inhibiting oncogene-induced senescence. Cancer Cell. 2011; 19:728–739. [PubMed: 21665147]
17. Guerra C, et al. Chronic pancreatitis is essential for induction of pancreatic ductal adenocarcinoma by K-Ras oncogenes in adult mice. Cancer Cell. 2007; 11:291–302. [PubMed: 17349585]
18. Liou GY, et al. Macrophage-secreted cytokines drive pancreatic acinar-to-ductal metaplasia through NF-kappaB and MMPs. J Cell Biol. 2013; 202:563–577. [PubMed: 23918941]

Author Manuscript Author Manuscript Author Manuscript Author Manuscript


19. De Lisle RC, Logsdon CD. Pancreatic acinar cells in culture: expression of acinar and ductal antigens in a growth-related manner. Eur J Cell Biol. 1990; 51:64–75. [PubMed: 2184038]
20. Crawford HC, Scoggins CR, Washington MK, Matrisian LM, Leach SD. Matrix metalloproteinase-7 is expressed by pancreatic cancer precursors and regulates acinar-to-ductal metaplasia in exocrine pancreas. J Clin Invest. 2002; 109:1437–1444. [PubMed: 12045257]
21. Sawey ET, Johnson JA, Crawford HC. Matrix metalloproteinase 7 controls pancreatic acinar cell transdifferentiation by activating the Notch signaling pathway. Proc Natl Acad Sci U S A. 2007; 104:19327–19332. [PubMed: 18042722]
22. Esni F, Miyamoto Y, Leach SD, Ghosh B. Primary explant cultures of adult and embryonic pancreas. Methods Mol Med. 2005; 103:259–271. [PubMed: 15542912]
23. Means AL, et al. Pancreatic epithelial plasticity mediated by acinar cell transdifferentiation and generation of nestin-positive intermediates. Development. 2005; 132:3767–3776. [PubMed: 16020518]
24. Cano DA, Hebrok M, Zenker M. Pancreatic development and disease. Gastroenterology. 2007; 132:745–762. [PubMed: 17258745]
25. Puri S, Hebrok M. Cellular plasticity within the pancreas--lessons learned from development. Dev Cell. 2010; 18:342–356. [PubMed: 20230744]
26. Chen LA, et al. PKD3 is the predominant protein kinase D isoform in mouse exocrine pancreas and promotes hormone-induced amylase secretion. J Biol Chem. 2009; 284:2459–2471. [PubMed: 19028687]
27. Miyamoto Y, et al. Notch mediates TGF alpha-induced changes in epithelial differentiation during pancreatic tumorigenesis. Cancer Cell. 2003; 3:565–576. [PubMed: 12842085]
28. Grippo PJ, Nowlin PS, Demeure MJ, Longnecker DS, Sandgren EP. Preinvasive pancreatic neoplasia of ductal phenotype induced by acinar cell targeting of mutant Kras in transgenic mice. Cancer Res. 2003; 63:2016–2019. [PubMed: 12727811]
29. Siveke JT, Einwachter H, Sipos B, Lubeseder-Martellato C, Kloppel G, Schmid RM. Concomitant pancreatic activation of Kras(G12D) and Tgfa results in cystic papillary neoplasms reminiscent of human IPMN. Cancer Cell. 2007; 12:266–279. [PubMed: 17785207]
30. Apelqvist A, et al. Notch signalling controls pancreatic cell differentiation. Nature. 1999; 400:877–881. [PubMed: 10476967]
31. Ringel J, et al. Aberrant expression of a disintegrin and metalloproteinase 17/tumor necrosis factor-alpha converting enzyme increases the malignant potential in human pancreatic ductal adenocarcinoma. Cancer Res. 2006; 66:9045–9053. [PubMed: 16982746]
32. Cheng P, et al. Notch-1 regulates NF-kappaB activity in hemopoietic progenitor cells. J Immunol. 2001; 167:4458–4467. [PubMed: 11591772]
33. Maniati E, et al. Crosstalk between the canonical NF-kappaB and Notch signaling pathways inhibits Ppargamma expression and promotes pancreatic cancer progression in mice. J Clin Invest. 2011; 121:4685–4699. [PubMed: 22056382]
34. Koch U, Lehal R, Radtke F. Stem cells living with a Notch. Development. 2013; 140:689–704. [PubMed: 23362343]
35. Trauzold A, et al. PKCmu prevents CD95-mediated apoptosis and enhances proliferation in pancreatic tumour cells. Oncogene. 2003; 22:8939–8947. [PubMed: 14654790]
36. Ferdaoussi M, et al. G protein-coupled receptor (GPR)40-dependent potentiation of insulin secretion in mouse islets is mediated by protein kinase D1. Diabetologia. 2012; 55:2682–2692. [PubMed: 22820510]
37. Harikumar KB, et al. A novel small-molecule inhibitor of protein kinase D blocks pancreatic cancer growth in vitro and in vivo. Mol Cancer Ther. 2010; 9:1136–1146. [PubMed: 20442301]
38. Guha S, Tanasanvimon S, Sinnett-Smith J, Rozengurt E. Role of protein kinase D signaling in pancreatic cancer. Biochem Pharmacol. 2010; 80:1946–1954. [PubMed: 20621068]
39. Kisfalvi K, Guha S, Rozengurt E. Neurotensin and EGF induce synergistic stimulation of DNA synthesis by increasing the duration of ERK signaling in ductal pancreatic cancer cells. J Cell Physiol. 2005; 202:880–890. [PubMed: 15389644]

Author Manuscript Author Manuscript Author Manuscript Author Manuscript


40. Shabelnik MY, Kovalevska LM, Yurchenko MY, Shlapatska LM, Rzepetsky Y, Sidorenko SP. Differential expression of PKD1 and PKD2 in gastric cancer and analysis of PKD1 and PKD2 function in the model system. Exp Oncol. 2011; 33:206–211. [PubMed: 22217708]
41. Yuan J, et al. Protein kinase d regulates cell death pathways in experimental pancreatitis. Front Physiol. 2012; 3:60. [PubMed: 22470346]
42. Yuan J, et al. Protein kinase D1 mediates NF-kappaB activation induced by cholecystokinin and cholinergic signaling in pancreatic acinar cells. Am J Physiol Gastrointest Liver Physiol. 2008; 295:G1190–1201. [PubMed: 18845574]
43. Yuan J, Rozengurt E. PKD, PKD2, and p38 MAPK mediate Hsp27 serine-82 phosphorylation induced by neurotensin in pancreatic cancer PANC-1 cells. J Cell Biochem. 2008; 103:648–662. [PubMed: 17570131]
44. Thrower EC, et al. A novel protein kinase D inhibitor attenuates early events of experimental pancreatitis in isolated rat acini. Am J Physiol Gastrointest Liver Physiol. 2011; 300:G120–129. [PubMed: 20947701]
45. Reichert M, et al. The Prrx1 homeodomain transcription factor plays a central role in pancreatic regeneration and carcinogenesis. Genes Dev. 2013; 27:288–300. [PubMed: 23355395]
46. Kopp JL, et al. Identification of Sox9-dependent acinar-to-ductal reprogramming as the principal mechanism for initiation of pancreatic ductal adenocarcinoma. Cancer Cell. 2012; 22:737–750. [PubMed: 23201164]
47. Stanger BZ, et al. Pten constrains centroacinar cell expansion and malignant transformation in the pancreas. Cancer Cell. 2005; 8:185–195. [PubMed: 16169464]
48. Jensen JN, Cameron E, Garay MV, Starkey TW, Gianani R, Jensen J. Recapitulation of elements of embryonic development in adult mouse pancreatic regeneration. Gastroenterology. 2005; 128:728–741. [PubMed: 15765408]
49. Kahlert C, et al. Increased expression of ALCAM/CD166 in pancreatic cancer is an independent prognostic marker for poor survival and early tumour relapse. Br J Cancer. 2009; 101:457–464. [PubMed: 19603023]
50. Gaida MM, et al. Expression of A disintegrin and metalloprotease 10 in pancreatic carcinoma. Int J Mol Med. 2010; 26:281–288. [PubMed: 20596609]
51. Sharlow ER, et al. Discovery of Diverse Small Molecule Chemotypes with Cell-Based PKD1 Inhibitory Activity. PLoS One. 2011; 6:e25134. [PubMed: 21998636]

Author Manuscript Author Manuscript Author Manuscript Author Manuscript

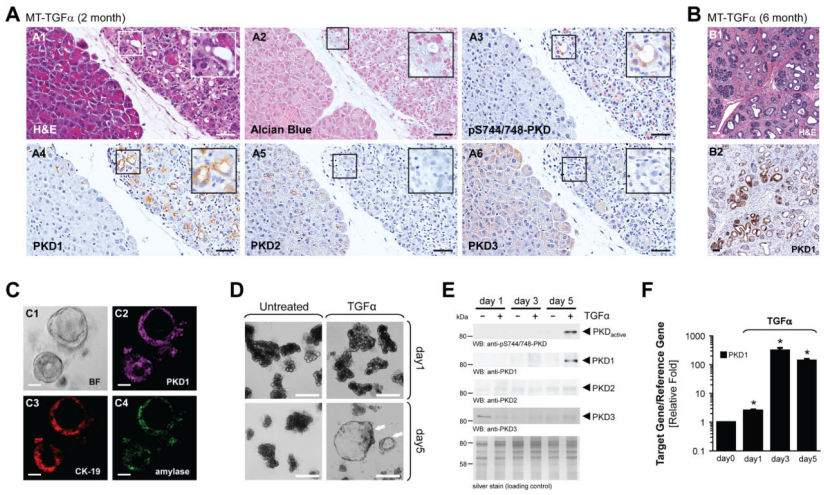


**Figure 1. PKD1 is upregulated in pancreatic acinar cells undergoing ADM**

(A, B) Pancreatic tissue (normal acinar area and regions with ADM, PanINs) from MT-TGFα transgene mice was stained with H&E, Alcian Blue, or analyzed by IHC for expression of PKD1 (anti-PKD1), PKD2 (anti-PKD2), PKD3 (anti-PKD3), or active PKD activity (anti-pS744/748-PKD), as indicated. The bar represents 50 μm. (C) Primary acinar cells were isolated from mouse pancreas and seeded in 3D culture in phenol red-free, growth factor-containing Matrigel. At day 5, expression of PKD1 (anti-PKD1, deep red), CK-19 (ductal marker, red) and amylase (acinar cell marker, green) were analyzed by immunofluorescence. BF = bright field. The bar represents 50 μm. (D–F) Primary acinar cells were isolated from mouse pancreas, seeded in 3D culture in collagen and transdifferentiation was induced with TGFα (50 ng $ml^{-1}$) as indicated. Ducts formed were photographed (D, bar represents 100 μm), isolated from the collagen and analyzed by Western blot for expression of PKD1, PKD2, PKD3, and active PKD (anti-S744/748-PKD) as indicated (E) or analyzed by QPCR for PKD1 expression (F). In (E) silver staining served as loading control. In (F), * indicates statistical significance ($p < 0.05$; student's *t*-test) as compared to control. Error bars (s.d.) were obtained from three experimental replicates. All experiments shown were performed at least 3 times with similar results.

Author Manuscript Author Manuscript Author Manuscript Author Manuscript

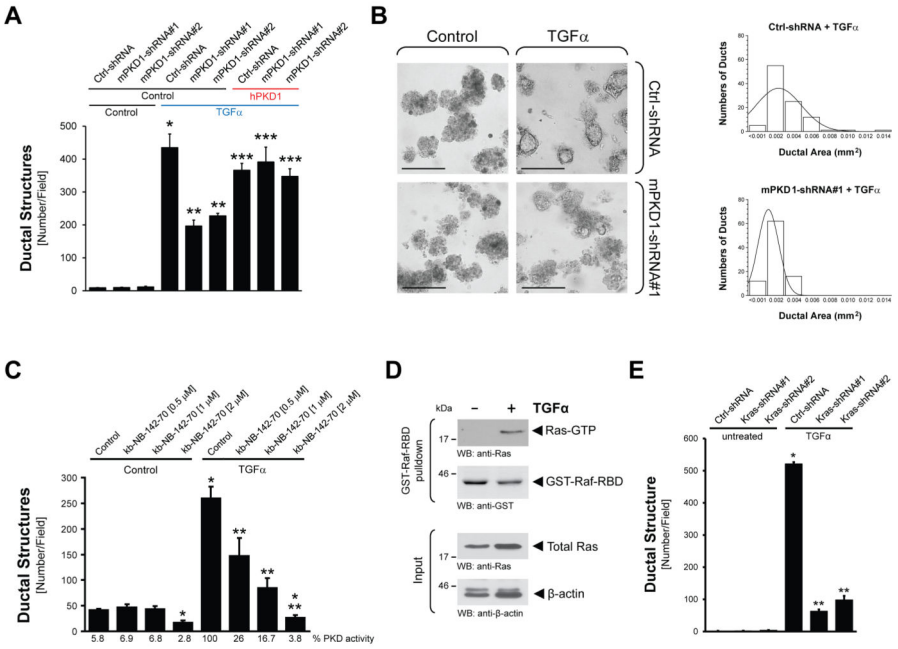


**Figure 2. PKD is necessary for TGFα-mediated metaplasia to ductal structures**

(A, B) Primary acinar cells were isolated from mouse pancreas and infected with lentivirus harboring (scrambled) control shRNA (Ctrl-shRNA) or 2 different sequences of PKD1-shRNA (#1, #2) specifically targeting mouse PKD1. In addition cells were lentivirally infected with human PKD1 or control virus, as indicated. Cells were then seeded in 3D culture in collagen and transdifferentiation was induced with TGFα (50 ng $ml^{-1}$). Formation of ductal structures was quantified (A), or ducts formed were photographed and the ductal area of 100 ducts was determined (B). In (B), the bar represents 200 μm. (C) Primary acinar cells were isolated from mouse pancreas, seeded in 3D culture in collagen, and transdifferentiation was induced with TGFα (50 ng $ml^{-1}$) in absence or presence of the PKD inhibitor kb-NB-142-70 at indicated doses. ADM events were quantified. (D) Primary acinar cells were isolated from mouse pancreas and stimulated with TGFα (50 ng $ml^{-1}$, 48 hours). Active Ras was pulled-down using GST-Raf-RBD. Samples were analyzed by SDS-PAGE and immunoblotting for pulled-down active Ras (anti-Ras), GST-Raf-RBD input (anti-GST), as well as other input controls (anti-Ras and anti-β-actin). (E) Primary acinar cells were isolated from mouse pancreas, infected with lentivirus harboring (scrambled) control shRNA (Ctrl-shRNA) or Kras-shRNA (2 different specific sequences, #1, #2), seeded in 3D culture in collagen and transdifferentiation was induced with TGFα (50 ng $ml^{-1}$). ADM events were quantified. In all figures, * indicates statistical significance ($p < 0.05$; student's *t*-test) as compared to control, ** indicates statistical significance ($p < 0.05$; student's *t*-test) as compared to TGFα treatment, *** indicates statistical significance ($p < 0.05$; student's *t*-test) as compared to respective shRNA sample. Error bars (s.d.) were obtained from three experimental replicates. All experiments shown were performed at least 3 times with similar results.

Author Manuscript Author Manuscript Author Manuscript Author Manuscript

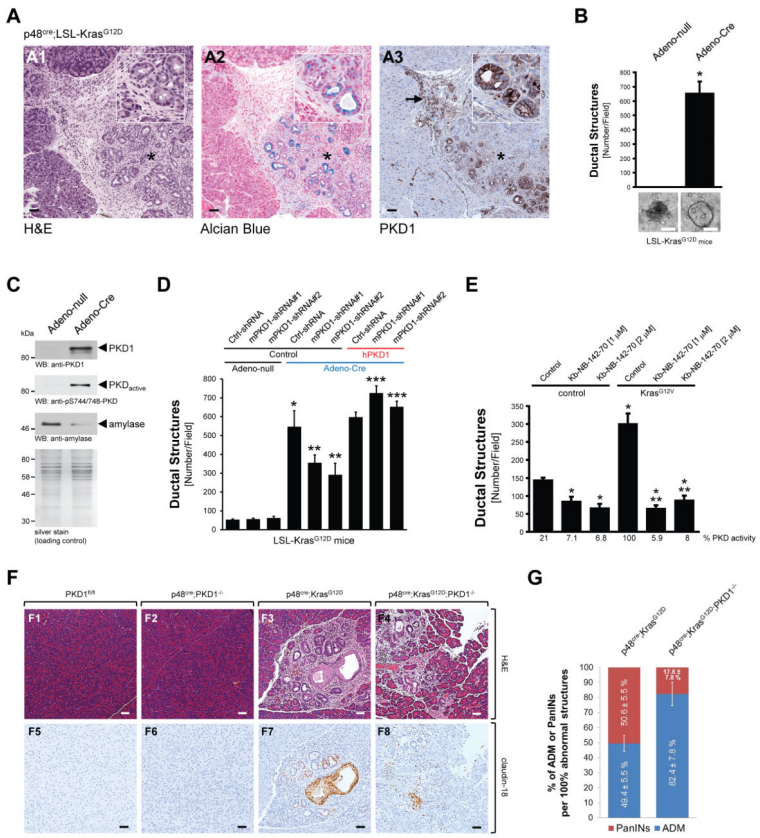


**Figure 3. PKD1 is necessary for Kras-induced metaplasia to ductal structures**

(A) Pancreatic tissue (normal acinar area and regions with ADM) from bi-transgenic p48$^{cre}$;Kras$^{G12D}$ mice was stained with H&E, Alcian Blue, or analyzed by IHC for PKD1 expression (anti-PKD1). The asterisk shows a typical region of newly-formed ductal structures. The arrow shows immune cells also staining positive for PKD1. The bar represents 50 μm. (B, C) Primary acinar cells were isolated from LSL-Kras$^{G12D}$ mice and infected with Adeno-Cre (or control virus) to induce expression of Kras$^{G12D}$. Formation of ductal structures was quantified and ducts formed were photographed (B), or ducts formed were isolated and analyzed by Western blot for PKD1 expression (anti-PKD1) or activity (anti-pS744/748) and anti-amylase (C). In (B) the bar represents 200 μm; in (C) silver staining served as loading control. (D) Primary acinar cells from LSL-Kras$^{G12D}$ mice were isolated from mouse pancreas and infected with lentivirus harboring (scrambled) control shRNA (Ctrl-shRNA) or 2 different sequences of PKD1-shRNA (#1, #2) specifically targeting mouse PKD1. Expression of mutant Kras was induced by adenoviral infection of cre-recombinase as indicated (Adeno-Cre), or Adeno-null as control. In addition cells were lentivirally-infected with human PKD1 or control virus as indicated. Cells were then seeded in 3D culture in collagen and formation of ductal structures was quantified. (E) Primary acinar cells were isolated from mouse pancreas, lentivirally-infected with Kras$^{G12V}$ and then seeded in 3D culture in collagen in absence or presence of the PKD inhibitor kb-NB-142-70 at indicated doses. Formation of ductal structures was quantified. In all figures, * indicates statistical significance ($p < 0.05$; student's *t*-test) as compared to control, ** indicates

Author Manuscript Author Manuscript Author Manuscript Author Manuscript

statistical significance ($p < 0.05$; student's *t*-test) as compared to stimulus, *** indicates statistical significance ($p < 0.05$; student's *t*-test) as compared to respective shRNA sample. Error bars (s. d.) were obtained from three experimental replicates. (F) Analysis of control, $p48^{cre}$;$Kras^{G12D}$ and $p48^{cre}$;$Kras^{G12D}$;$PKD1^{-/-}$ mice for regions of ADM/PanIN using H&E staining and IHC for claudin-18. Additional controls are depicted in Supplementary Fig. 3. The bar represents 50 μm. (G) Quantitation of ADM and PanIN lesions in $p48^{cre}$;$Kras^{G12D}$ and $p48^{cre}$;$Kras^{G12D}$;$PKD1^{-/-}$ mice.

Author Manuscript Author Manuscript Author Manuscript Author Manuscript

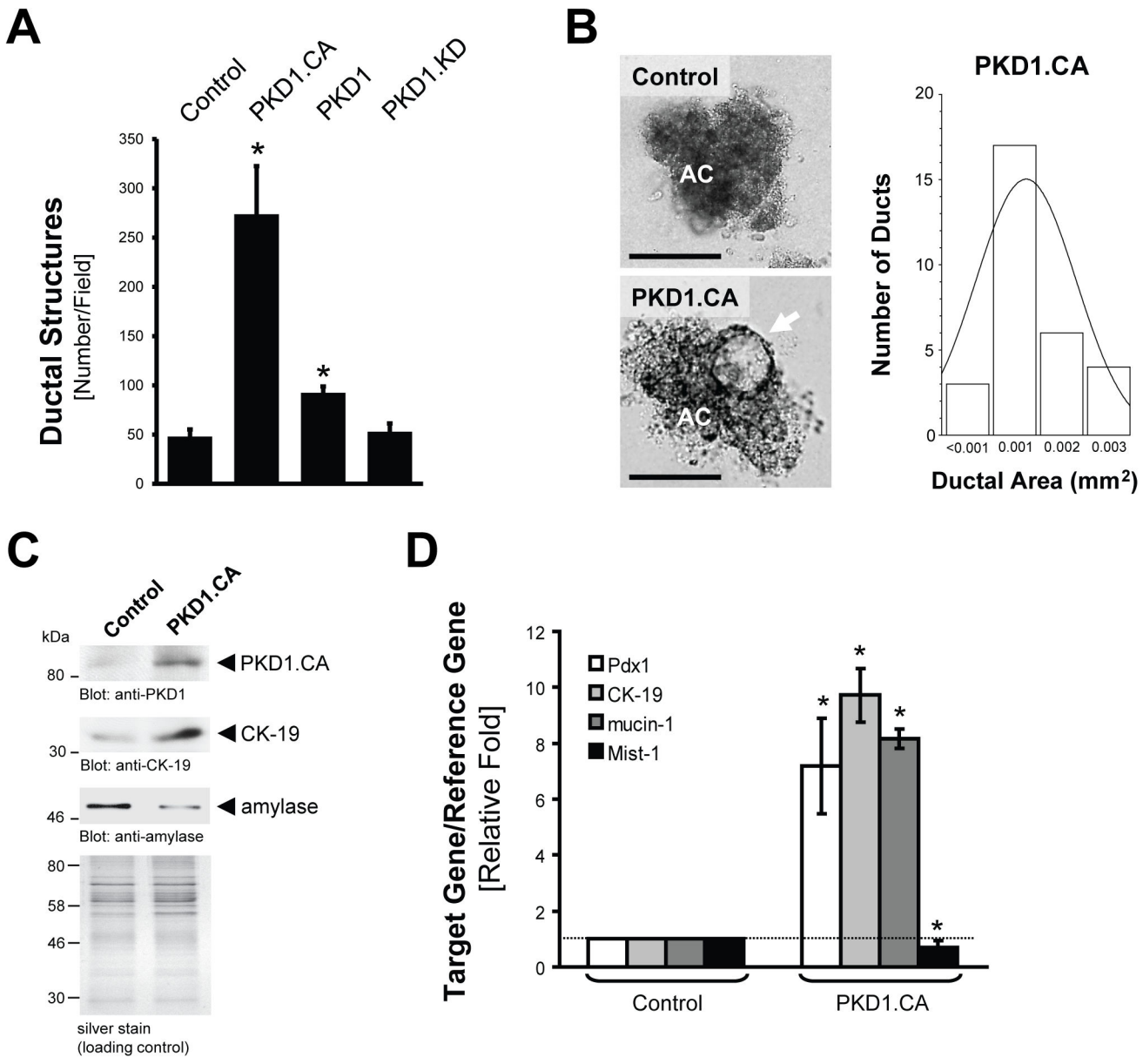


**Figure 4. Active PKD1 is sufficient to drive the formation of duct-like structures**

(A) Primary acinar cells were isolated from mouse pancreas, infected with lentivirus harboring control, wildtype PKD1, active PKD1 (PKD1.CA), or kinase-dead PKD1 (PKD1.KD) and seeded in collagen 3D culture. At day 7, ductal structures formed were quantified. (B–D) Primary acinar cells were isolated from mouse pancreas, infected with lentivirus harboring control or active PKD1 (PKD1.CA) and seeded in collagen 3D culture. At day 7, ductal structures formed were photographed and ductal area (n=30) determined (B, the bar represents 100 μm). AC = acinar cells; the arrow indicates duct-like structure. Additionally, ducts were isolated and analyzed for markers of transdifferentiation (anti-CK-19, anti-amylase) and expression of active PKD1 using Western blot (C) or for markers of acinar cell de- and transdifferentiation (Pdx1, Mist-1, CK-19, mucin-1) using quantitative

Author Manuscript Author Manuscript Author Manuscript Author Manuscript

PCR (D). In all figures, * indicates statistical significance ($p < 0.05$; student's *t*-test) as compared to control. Error bars (s. d.) were obtained from three experimental replicates. All experiments shown were performed at least 3 times with similar results.

Author Manuscript Author Manuscript Author Manuscript Author Manuscript

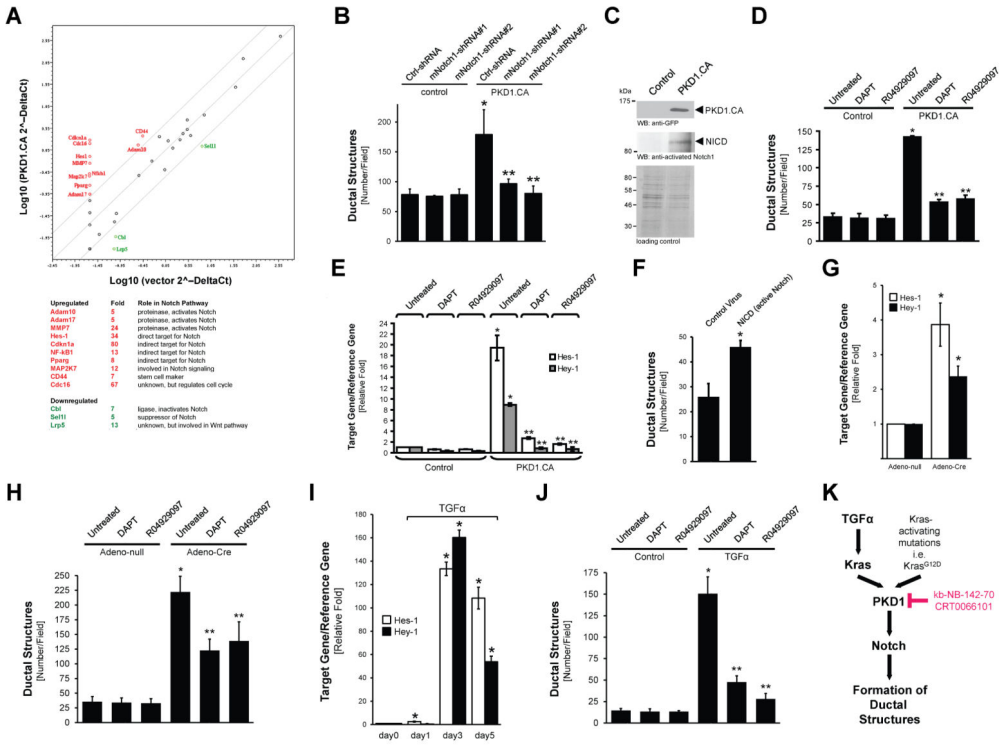


**Figure 5. PKD1 mediates formation of duct-like structures through Notch**

(A) Scatter plot showing fold changes in expression of genes in control primary acinar cells or cells expressing constitutively-active PKD1 (PKD1.CA). The center line indicates no difference between the expression of genes under both conditions. The side lines indicate a 4-fold difference in either direction. The genes expressed more than 4-fold in the PKD1.CA group as compared to the control group are labeled in red. The genes expressed lower than 4-fold in the PKD1.CA group are labeled in green. Their role in the Notch pathway as well as fold change is provided in the table. (B) Primary acinar cells were isolated from mouse pancreas and infected with lentivirus harboring (scrambled) control shRNA (Ctrl-shRNA) or 2 different sequences of Notch1-shRNA (#1, #2) specifically targeting mouse Notch1. In addition cells were lentivirally-infected with active PKD1 (PKD1.CA) or control virus as indicated. Cells were then seeded in 3D culture in collagen and formation of ductal structures was quantified. (C) Primary acinar cells were isolated from mouse pancreas and lentivirally-infected with control or GFP-tagged active PKD1 (PKD1.CA; PKD1.S738E/S742E mutant). Cells were then seeded in 3D culture in collagen. At day 6, cells were re-isolated and analyzed by Western bot for activated Notch 1 fragment (NICD). Expression of PKD1.CA was controlled by Western blot against GFP. Silver staining served as a loading control. (D, E) After isolation and infection with control or PKD1.CA harboring lentivirus, primary acinar cells were seeded in collagen 3D culture in absence or presence of the γ-secretase inhibitors DAPT (5 μM) or R04929097 (10 nM) as indicated. At day 6, formation of ductal-structures was determined (D), or cells were isolated from the collagen and analyzed by quantitative PCR for expression of the Notch target genes Hes-1 and Hey-1 (E). (F) Primary acinar cells were isolated from mouse pancreas and infected with lentivirus harboring an active Notch fragment (NICD) or control virus. Cells were then seeded in 3D

Author Manuscript Author Manuscript Author Manuscript Author Manuscript

culture in collagen and formation of ductal structures was quantified. (G, H) Primary acinar cells from LSL-Kras$^{G12D}$ mice were isolated from mouse pancreas and expression of mutant Kras was induced by adenoviral infection of cre-recombinase as indicated (Adeno-Cre; or Adeno-null as control). Cells then were seeded in collagen 3D culture in absence or presence of the γ-secretase inhibitors DAPT (5 μM) or R04929097 (10 nM) as indicated. At day 6, cells were isolated from the collagen and analyzed by quantitative PCR for expression of the Notch target genes Hes-1 and Hey-1 (G), and formation of ductal-structures was determined (H). (I, J) Primary acinar cells were seeded in collagen 3D culture in absence or presence of TGFα (50 ng ml$^{-1}$) and the γ-secretase inhibitors DAPT (5 μM) or R04929097 (10 nM) as indicated. At indicated days, cells were isolated from the collagen and analyzed by quantitative PCR for expression of the Notch target genes Hes-1 and Hey-1 (I), and formation of ductal-structures was determined (J). In all figures shown in B, D–J, * indicates statistical significance ($p < 0.05$; student's *t*-test) as compared to control, ** indicates statistical significance ($p < 0.05$; student's *t*-test) as compared to stimulus. Error bars (s. d.) were obtained from three experimental replicates. (K) Schematic of a TGFα- and Kras-induced PKD1-Notch signaling pathway that drives formation of pancreatic duct-like structures and PanIN formation. All experiments shown were performed at least 3 times with similar results.